Ring Currents in the Dismutational Aromatic Si6R6

ARTICLE *in* ANGEWANDTE CHEMIE INTERNATIONAL EDITION · DECEMBER 2010

Impact Factor: 11.26 · DOI: 10.1002/anie.201003988 · Source: PubMed

3 AUTHORS, INCLUDING:

Raphael Johann Friedrich Berger
University of Salzburg
77 PUBLICATIONS **640** CITATIONS
SEE PROFILE

David Scheschkewitz
Universität des Saarlandes
99 PUBLICATIONS **1,500** CITATIONS
SEE PROFILE

Silicon Clusters

DOI: 10.1002/anie.201003988

Ring Currents in the Dismutational Aromatic Si_6R_6**

Raphael J. F. Berger, Henry S. Rzepa, and David Scheschkewitz*

In memory of Marie-Madeleine Rohmer

Partially hydrogenated silicon clusters are intermediates in nucleation processes during the deposition of elemental silicon from the gas phase by the decomposition of silane vapors.[1] In addition, residues of such clusters in bulk materials are thought to be determining factors for the optoelectronic properties of hydrogenated amorphous and porous silicon films.[2] In order to elucidate the bonding situations and relative stabilities, substantial efforts in terms of computations[3] and experimental gas-phase studies[4] have thus been directed towards subvalent clusters Si_nH_m ($n = 4$–100, $m < n$). Frequently recurring features, irrespective of cluster size, are the "naked" vertices with hemispheroidal tetracoordination in which all bonds point to one side (Scheme 1).[1–4]

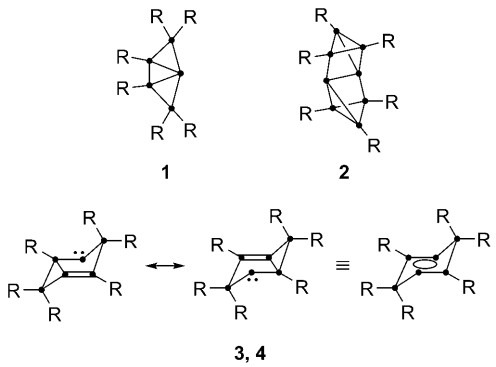

Scheme 1. Neutral silicon clusters **1** and **2** with tetracoordinated "naked" vertices, and dismutational isomers **3** and **4** of hexasilabenzene (● = silicon; **1**, **3**: R = Tip = 2,4,6-*i*Pr$_3$C$_6$H$_2$; **2**: R = Si*t*Bu$_3$; **4**: R = H).

Isolable neutral compounds with "naked" atoms stabilized by sterically demanding substituents at the remaining vertices, which could help to attain a better understanding of structure–property relationships, are scarce in the case of silicon. Until recently, only the Si_5R_6 derivative **1**[5] and an Si_8R_6 cluster **2** were known.[6] Even the more widely available derivatives of germanium, tin, and lead (also referred to as "metalloid" when the average oxidation number is between 0 and +I) have so far hardly allowed for the deduction of general rules regarding structure and bonding.[7] Hence, while Group 14 cluster anions of the Zintl type usually obey the Wade–Mingos rules[8] and are prime examples of spherical aromaticity,[9] the electronic situation is often less clear-cut in the case of neutral partially substituted derivatives.[7]

Recently, some of us reported the isolation and structural characterization of an isomer of hexasilabenzene, Si_6Tip_6 (**3**, Tip = 2,4,6-triisopropylphenyl), which features a Si_6 scaffold with two unsubstituted, two mono-, and two disubstituted silicon atoms and hence displays the key features of partially substituted silicon clusters.[10,11] The experimentally determined inversion-symmetric structure and the surprising thermal stability of **3** suggested an unusual bonding situation. This prompted theoretical calculations, and on this basis a formerly unknown type of aromaticity was proposed for this closed-shell compound. The term "dismutational aromaticity" was introduced accounting for the formalism of intramolecular disproportionation ("dismutation") of four of the silicon(I) centers of the isomeric Hückel-aromatic hexasilabenzene to generate **3**.[10]

An aspect of aromaticity that is readily observable experimentally by NMR spectroscopy is the strong magnetic deshielding of atoms that participate in the aromatic ring current of a molecule. Therefore, while the observed ^{29}Si NMR chemical shifts for the silicon atoms in **3** with one substituent at $\delta = 125$ ppm (Si2 and Si2′, see Figure 1) are as expected, the strong highfield shift of atoms Si3 and Si3′ at $\delta =$

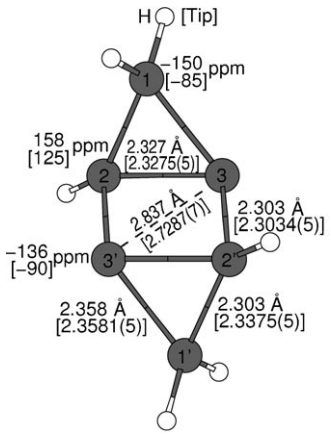

Figure 1. Calculated[12] [and experimentally determined[10]] interatomic distances and ^{29}Si chemical shifts of Si_6H_6 (**4**) [Si_6Tip_6 (**3**)]. Both structures show C_i symmetry.

[*] Dr. R. J. F. Berger
Fakultät für Chemie, Universität Bielefeld
33615 Bielefeld (Germany)
Fax: (+49) 521-106-6164
E-mail: raphael.berger@uni-bielefeld.de
Prof. H. S. Rzepa, Dr. D. Scheschkewitz
Department of Chemistry, Imperial College London
London SW7 2AZ (United Kingdom)

[**] Funding by the Aventis Foundation (Karl-Winnacker Fellowship to D.S.) is gratefully acknowledged.

−90 ppm (see Figure 1) is puzzling, particularly in view of the calculated NICS(0) value of $\delta = -24$ ppm at the center of symmetry, which supports a strong aromatic character of the silicon framework (benzene $\delta \approx 10$ ppm).

In order to rationalize these seemingly contradictory results and to shed more light onto the origins of the aromatic properties of **3**, we have investigated the magnetically induced probability current density field ($\mathbf{J^B}$) topology of a simplified model compound of **3**; in the isostructural hexasilabenzene (Si_6H_6) isomer **4** all organic substituents are replaced by hydrogen atoms (Figure 1).[11–13] Moreover we want to advocate the usage of the topology of $\mathbf{J^B}$ as an intuitive but also clearly defined property for the classification of aromatic compounds and molecular aromaticity.

$\mathbf{J^B}$ has very appealing properties for the investigation and analysis of compounds showing delocalized bonding situations. 1) All anisotropic (a fixed orientation of molecule in the magnetic field) magnetic field properties (like the susceptibility) can be calculated in a straightforward fashion from $\mathbf{J^B}$ simply on basis of the classical electrodynamic Maxwell equations.[14] 2) A visual inspection of the $\mathbf{J^B}$ field gives a quick overview of "how the currents flow" in a molecule, which give rise to exactly the observed magnetic shielding properties by (back-) inducing magnetic fields.[15] 3) $\mathbf{J^B}$ satisfies a local continuity condition of charge conservation;[16] consequently the field can be represented graphically, for instance, in the form of closed loops (streamlines).[17] 4) Some general mathematical and physical laws for the electronic current density topology have been derived, simplifying the topological analysis to a large extent.[15,16] 5) If one is willing to accept that "delocalized bonds" are the origin of molecular magnetic response properties, the magnetically induced ring-current densities can be regarded as "footprints" of bond delocalization.

As an example of a ring current topology, in Figure 2 some representative $\mathbf{J^B}$ vectors from the molecular plane of a benzene molecule are shown. The magnetic field vectors in this work are set perpendicular to the plane of the paper and point upwards. Figure 2a shows the numerically calculated $\mathbf{J^B}$ vectors, and Figure 2b shows a representation similar to that used below in the analysis of **4**. The most important topological features are the points where $\mathbf{J^B}$ vanishes [$\mathrm{mod}(\mathbf{J^B}) = 0$], the so-called stagnation points (SPs).[16] Three different types of SPs are depicted in Figure 2b: a vortex SP in a diamagnetic vortex with a clockwise current (I), a paramagnetic vortex SP with a counterclockwise vortex (II), and a saddle SP (III) occurring at an osculation point of four vortices.

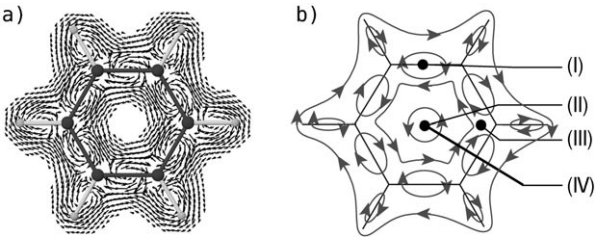

Figure 2. a) Representative magnetically induced probability current density ($\mathbf{J^B}$) vectors in the molecular plane of a benzene molecule. The magnetic field vector points out of the plane of the paper. Very large and very small vectors are omitted. b) Schematic depiction of current vortices from (a). (I) shows a diamagnetic vortex, where the black dot is located at the stagnation point (SP), (II) marks a paramagnetic vortex SP, and (III) a current saddle SP; the bold line (IV) represents a half-plane delimited by the axis of symmetry. The currents flowing through this plane integrate to 15 nAT^{-1} diamagnetic and -5 nAT^{-1} paramagnetic contributions, resulting in an overall diamagnetic ring current of 10 nAT^{-1} for benzene, a value that can be considered as typical for the presence of Hückel-type $6e^-$ aromaticity.[13]

All the existing SPs for one molecule and one **B**-field orientation are called a stagnation graph (SG)[16] A molecular stagnation graph always contains a connected set of points, the primary graph, originating from a primary vortex at a far distance from the molecule (which is either dia- or paramagnetic).[16] The SPs in the primary graph usually are connected roughly along the **B** field. The SG may contain other disconnected graphs and may also contain isolated points. The whole SG uniquely characterizes the complete topology of $\mathbf{J^B}$ originating from a certain **B** field.[16]

In order to investigate the nature of $\mathbf{J^B}$ in **4**, its geometry was optimized using a correlated ab initio method (MP2).[11] The resulting structure parameters are partly in excellent agreement with corresponding parameters found in the solid-state structure of **3**, while the agreement in isotropic nuclear magnetic shielding constants is only qualitatively satisfying (see Figure 1). The differences must be assigned to the formal replacement of Tip in **3** with H in the model compound **4**. This is evident from the good agreement of calculated and experimental shielding parameters in reference [[10]]. In order to investigate the topology of $\mathbf{J^B}$, the direction of the magnetic field was defined to be perpendicular to the plane *p* defined by Si2-Si3-Si2′-Si3′. Sample vectors of $\mathbf{J^B}$ from planes parallel to *p* in different distances from 3 to −3 bohr in steps of 1 bohr (≈ 0.53 Å), to *p* are shown in Figure 3a–g. The depicted vectors are selected from a range that excludes the large currents from the strong diamagnetic spherical currents (loops γ in Figure 3h, vide infra) originating from filled atomic subshells[18] [$\mathrm{mod}(\mathbf{J^B}) > 2$ nAT^{-1}] and also very small vectors [$\mathrm{mod}(\mathbf{J^B}) < 0.2$ nAT^{-1}]. Consequently, the representations show only the most substantial vectors originating mostly from the valence electrons. In Figure 3h a schematic diagram summarizing the observed current loops is given.

The dominating ring-current contribution can be assigned to the diamagnetic (clockwise in Figure 3) loop α, which includes both of the unsubstituted Si atoms (Si3, Si3′) but excludes the monosubstituted Si atoms Si2 and Si2′. From this picture it is evident that Si3 and Si3′ are strongly magnetically shielded owing to the diamagnetic current loop α. The two closed loops β circulate in a counterclockwise orientation around atoms Si2 and Si2′ but in a clockwise orientation around Si3 and Si3′. Therefore, while atoms Si3 and Si3′ are additionally shielded by the β loop, Si2 and Si2′ are deshielded owing to a locally counterclockwise orientation of the β loop in their proximity. Together with the circumvention of Si2 and Si2′ by the α loop, this explains the large difference in ^{29}Si NMR chemical shifts in atoms Si2(2′) and Si3(3′). In addition, loop α influences the magnetic field at atoms Si1 and Si1', which both point into the domain of the

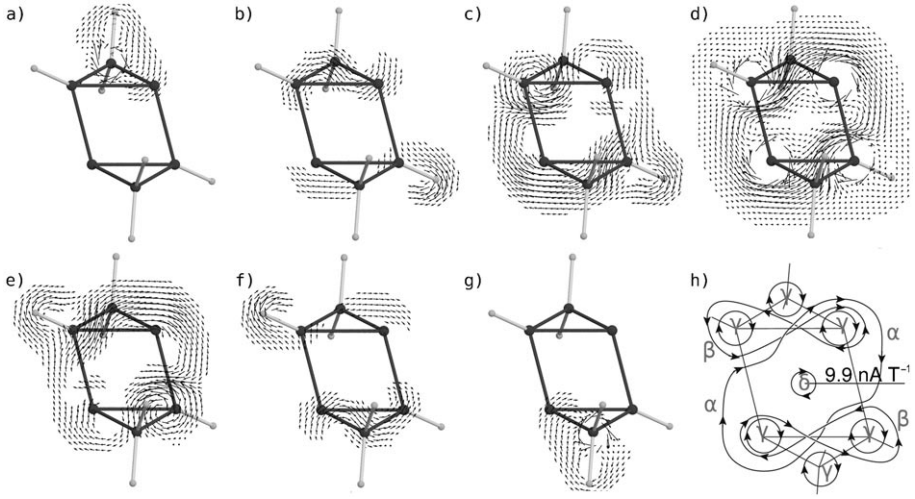

Figure 3. Planes cut parallel to the Si2-Si3-Si2′-Si3′ plane (*p*) showing magnetically induced current densities in **2** when a homogeneous **B** field is applied perpendicular and at a distance of *z* to *p*. Selected vectors representing the largest contribution of the currents densities from the valence electrons are shown. a) $z = 1.61$ Å, b) $z = 1.06$ Å, c) $z = 0.53$ Å, d) $z = 0$ Å, e) $z = -0.53$ Å, f) $z = -1.06$ Å, g) $z = -1.61$ Å. h) Representation of the most significant part of the total valence electron current density. The total ring current integrates to 9.9 nAT^{-1} (10.1 nAT^{-1} is the diamagnetic and 0.2 nAT^{-1} is the paramagnetic contribution). The vortices labeled with Greek letters are discussed in the text.

loop resulting in their highfield ^{29}Si NMR shifts. Small differences between **3** and **4** in the position of Si1(Si1′) relative to loop α might thus have a substantial influence on the observed magnetic shielding. This explains to a large extent the non-negligible differences between the experimentally observed and calculated chemical shielding parameters in **3** and **4**, which are largest for Si1 and Si1′ ($\Delta\delta = 65$ ppm).

The numerical integration of $\mathbf{J^B}$ over a half-plane (symbolized by the black line in Figure 3h) cutting the molecule parallel to the *z* axis through its center of inversion yields a diamagnetic current contribution of 10.1 nAT^{-1} and an almost vanishing paramagnetic current contribution of -0.2 nAT^{-1}. Overall, the magnetically induced ring current is diamagnetic and amounts 9.9 nAT^{-1}, which is approximately the same as in benzene and hence indicates the presence of a magnetically induced ring current typical in size for aromatic molecules. Most remarkably, within this integration scheme there is almost no paramagnetic contribution to the total current. Moreover, the central vortex δ is diamagnetic as well. This is in complete contrast to the ring-current topology of benzene and in general must contrast with the ring-current topologies of all planar aromatic molecules of D_{nh} symmetry. It can easily be proven on a mathematical basis that in all such molecules a paramagnetic central vortex must exist (for instance benzene as depicted in Figure 2).[15] Consequently, the nonplanar **3** and **4**, containing the planar Si2-Si3-Si2′-Si3′ moieties, cannot be classified as instances of planar aromatic or analogous compounds. The fact that the integrated induced total currents flowing through **4** and through benzene are practically equal (both roughly -10 nAT^{-1}), while the respective NICS(0) values are more than twice as large in **4** (-24 ppm) than in benzene (-10 ppm) can be explained by the occurrence of the central paramagnetic vortex in common planar aromatic molecules, which always counteracts to some extent their magnetic shielding, and locally especially in the NICS(0) reference point in the ring center. This important caveat for the consideration of NICS values was first stated by Lazeretti.[17]

Our findings exclude the classification of **4** and **3** as $6e^-$ Hückel-aromatic analogues since there is no central paramagnetic vortex, this being a necessary condition for the presence of planar aromaticity. Moreover, such paramagnetic vortices are also present in nonplanar Hückel-aromatic analogues (homoaromatic compounds)[18] such as the homotropylium and the 1,3-bishomotropylium cations. In this way chemically analogous compounds share the topological characteristics of $\mathbf{J^B}$. In fact, the presence of a central diamagnetic vortex in **3** and **4** is much more reminiscent of the situation in spherical aromatic compounds[9,19] such as P_4 and P_3As.[20]

On the basis of our findings we advocate the analysis of the magnetically induced probability current density field topology as a tool for the systematic and strict categorization of aromatic compounds. Further investigations including a detailed topological analysis based on the generation and evaluation of stagnation graphs[16,17] of **3** and **4** as well as related compounds are currently in progress.

Received: June 30, 2010
Published online: November 16, 2010

Keywords: cluster compounds · magnetically induced ring currents · NMR spectroscopy · silicon · topology

[1] For example, a) M. T. Swihart, S. L. Girshik, *J. Phys. Chem. B* **1999**, *103*, 64; b) M. Shiratani, K. Koga, Y. Watanabe, *Thin Solid Films* **2003**, *427*, 1; c) W. M. Nakamura, H. Miyahara, K. Koga, M. Shiratani, *J. Phys. Conf. Ser.* **2008**, *100*, 082018; d) N. Ning, S. M. Rinaldi, H. Vach, *Thin Solid Films* **2009**, *517*, 6234; e) N. Ning, H. Vach, *J. Phys. Chem. A* **2010**, *114*, 3297.

[2] For example, a) T. V. Torchynska, *Superlattices Microstruct.* **2009**, *45*, 267; b) M. Lopez del Puerto, M. Jain, J. R. Chelikowsky, *Phys. Rev. B* **2010**, *81*, 035309; c) Ye. S. Shcherbyna, T. V. Torchynska, *Thin Solid Films* **2010**, *518*, S204.

[3] For example, a) D. K. Yu, R. Q. Zhang, S. T. Lee, *J. Appl. Phys.* **2002**, *92*, 7453; b) M. Tang, C. Z. Wang, W. C. Lu, K. M. Ho, *Phys. Rev. B* **2006**, *74*, 195413; c) X.-J. Li, C.-P. Li, J.-C. Yang, A. F. Jalbout, *Int. J. Quantum Chem.* **2009**, *109*, 1283; d) A. D. Zdetsis, *Phys. Rev. B* **2009**, *79*, 195437.

[4] a) S. D. Chambreau, L. Wang, J. Zhang, *J. Phys. Chem. A* **2002**, *106*, 5081; b) S. J. Peppernicka, K. D. D. Gunaratneb, A. W. Castleman, Jr., *Int. J. Mass Spectr.* **2010**, *290*, 65.
[5] D. Scheschkewitz, *Angew. Chem.* **2005**, *117*, 3014; *Angew. Chem. Int. Ed.* **2005**, *44*, 2954.
[6] G. Fischer, V. Huch, P. Mayer, S. K. Vasisht, M. Veith, N. Wiberg, *Angew. Chem.* **2005**, *117*, 8096; *Angew. Chem. Int. Ed.* **2005**, *44*, 7884.
[7] Review: A. Schnepf, *Chem. Soc. Rev.* **2007**, *36*, 745.
[8] Review: S. Sevov, J. M. Goicoechea, *Organometallics* **2006**, *25*, 5678.
[9] a) Z. Chen, A. Hirsch, S. Nagase, W. Thiel, P. von R. Schleyer, *J. Am. Chem. Soc.* **2003**, *125*, 15507; b) Z. Chen, S. Neukermans, X. Wang, E. Janssens, Z. Zhou, R. E. Silverans, R. B. King, P. von R. Schleyer, P. Lievens, *J. Am. Chem. Soc.* **2006**, *128*, 12829.
[10] K. Abersfelder, A. J. P. White, H. S. Rzepa, D. Scheschkewitz, *Science* **2010**, *327*, 564.
[11] The MP2/TZVPP level of theory implemented in TURBOMOLE[12] was used throughout this work in connection with standard parameter settings recommended for the calculation of NMR shielding constants at this level of theory. GIMIC[13] was used for the numerical calculation and integration of $\mathbf{J}^{\mathbf{B}}$.
[12] Turbomole 5.10, R. Ahlrichs, M. Bär, M. Häser, H. Horn, C. Kölmel, *Chem. Phys. Lett.* **1989**, *162*, 165.
[13] J. Jusélius, D. Sundholm, J. Gauss, *J. Chem. Phys.* **2004**, *121*, 3952.
[14] J. O. Hirschfelder, *J. Chem. Phys.* **1978**, *68*, 5151.
[15] S. Pelloni, F. Faglioni, R. Zanasi, P. Lazzeretti, *Phys. Rev. A* **2006**, *74*, 012506.
[16] J. A. N. F. Gomes, *Phys. Rev. A* **1983**, *28*, 559.
[17] P. Lazzeretti, *Prog. Nucl. Magn. Reson. Spectrosc.* **2000**, *36*, 1.
[18] Q. Zhang, S. Yue, X. Lu, Z. Chen, R. Huang, L. Zheng, P. v. R. Schleyer, *J. Am. Chem. Soc.* **2009**, *131*, 9789.
[19] M. Reiher, A. Hirsch, *Chem. Eur. J.* **2003**, *9*, 5442.
[20] B. M. Cossairt, C. C. Cummins, A. R. Head, D. L. Lichtenberger, R. J. F. Berger, S. A. Hayes, N. W. Mitzel, G. Wu, *J. Am. Chem. Soc.* **2010**, *132*, 8459.

